Excitation cross-sections of the praseodymium atom

Yu. Smirnov

Classification
Physics Abstracts
34.80D

Excitation cross-sections of the praseodymium atom

Yu. M. Smirnov

Moscow Power Engineering Institute, Krasnokazarmennaja str. 14, Moscow 111250, Russia

(Received 30 November 1992, revised 14 June 1993, accepted 1 October 1993)

Abstract . — Excitation cross-sections of PrI were measured at an electron energy 30 eV for 82 spectral lines. We have used the method of extended crossing beams with detection of the optical signal. For half of the total number the energy dependences were measured in the electron energy range of 0...200 eV. The largest measured excitation cross-sections reach (5-8) $\times 10^{-16}$ cm^2. A classification is suggested for 18 previously unclassified lines.

1. Introduction.

During the last years the field of application of rare-earth elements has enlarged considerably, and interest in their properties has acquired, beside general scientific, essentially applied character as well. This growth applies to properties of rare-earth metal atoms both in solid and in gaseous phase. Nevertheless, atomic constants, including cross-sections of inelastic collisions with electrons, for many atoms of rare-earth elements are still unknown or are rather limited in number. Up to now, inelastic collisions of the praseodymium atom with slow electrons have not been studied either experimentally, or theoretically.

2. Experiment.

In the present paper a method of extended crossing beams [1] is used for the measurement of excitation cross-sections of the praseodymium atom with electrons of low and medium energies (0...200 eV). The method of extended crossing beams, suggested in 1969, aims at improving informativity of the traditional method of crossing beams by means of enlarging the volume of intersection region, where interaction between particles takes place. In our experiments this volume amounts to 70 cm^3, whereas in most analogous experiments of other researchers it is less than 1 cm^3. This difference in volumes by 2-3 decimal orders with preserved values of atom concentration and current density of electron beam, naturally, leads to increasing the level of the optical signal by 2-3 orders.

Taking into consideration that the detection systems used in such experiments, work at the limits of capabilities of modern equipment, it must be admitted that other methods of improving informativity of experiments with crossing beams are hardly possible at present. The increase of atom concentration above a certain value is inadmissible, since the role of interaction between heavy particles becomes more significant, which distorts results of the experiment. Increasing the current density in the electron beam leads to considerable deterioration of the monokinetic properties of electrons because of their space charge influence, which is also unacceptable. There are significant reserves in increasing the collection of radiation of excited atoms. Thus, the most realistic way of improving the informativity of the crossing beams method – increasing the number of interacting particles without increasing the density of atom and electron flows is implemented in the method of extended crossing beams. Unfortunately, it is difficult to apply this method for measuring differential (depending on the angle) scattering cross-sections, but when the detection of an optical signal is used in the traditional scheme of such experiments, it allows the improvement of the signal/noise ratio by more than 2 decimal orders. The equipment and technique of the experiment were considerably perfected during 1980-1983 [1].

The diagram of the apparatus with extended crossing beams is shown in figure 1. The parts are numbered one through is. The total vacuum volume is divided by water-cooled diaphragms (5) into four sections, from which air is evacuated differentially. The electron beam (1) is directed from the melting electron gun to the surface of studied metal (3), placed in the copper crucible 2, cooled by an intensive water flow, as well as to the graphite base or tantalum cup. Diaphragms (5) form the atom beam (4), which has in the region of intersection with the electron beam (14) transverse dimensions 26×200 mm and a divergence angle with the plane near 40°. After passing the interaction region the atom beam condenses on the water-cooled panel (6).

For the source of an electron beam we use a special low-voltage electron gun with a flat oxide-coated cathode (8) with indirect heating, which has an emitting surface 13×200 mm. Inside the cathode body there is an alundum-coated tungsten heater (7). To control grid (9) square pulses with frequency 830 Hz and pulse ratio 2 are applied, which provides modulation of density of the electron beam current with 100 % depth. An accelerating voltage is applied between the cathode and the second grid (10); it is fixed while recording spectra and it smoothly changes from zero to maximum value while recording optical excitation functions. After crossing the atom beam the electron beam (14) is collected by a double collector; the external collector (12) has a potential of the collision space, and a positive voltage up to + 15 V is applied to the internal collector (11) for collecting scattered and secondary emitted electrons.

The distribution of the potential in the collision space created by the space charge of the beam, is found to be one of the most important factors, influencing the monokinetic feature of the electron beam. This factor is also of importance in the traditional variant of the crossing beams method (unfortunately, corresponding estimate are published extremely seldom), but its role becomes determining in case of extended beams. In figure 2 current-voltage characteristics of the low-voltage electron gun with extended beam are shown for three cases: 1) long path grid 2-collector, 2) short path grid 2-collector (but in this case it is practically impossible for the atom beam to get through the collision space) and 3) big path grid 2-collector plus quasi-equipotentialization is applied.

By the last term we denote the suggested method and implemented method, adopted by us for smoothing the potential pattern in extended beams of low-energy electrons. To achieve this aim we stretch in the collision space tungsten strings (13) with spacings 4×4 mm and diameter 26...33 μm, oriented parallel to the line of sight of the optical system (that is perpendicular to the drawing plane in Fig. 1). These strings, fixed on metal supports, are compulsorily

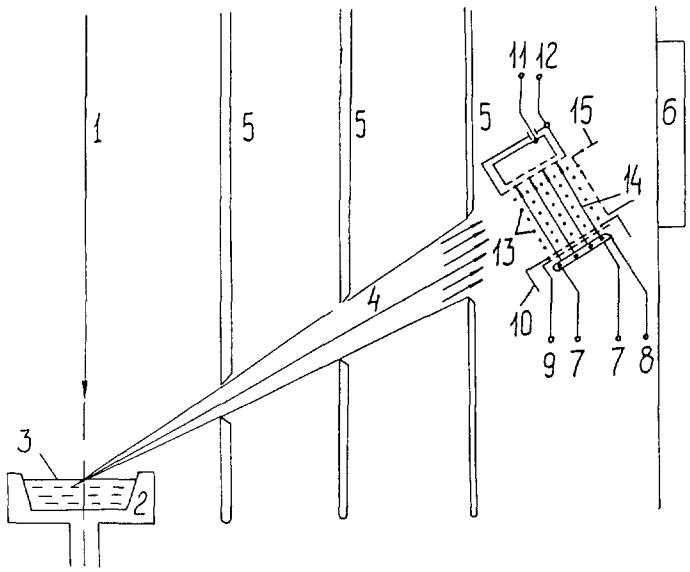

Fig. 1. — Diagram of the plant with extended crossing beams. (1) electron beam for melting of metal; (2) crucible; (3) evaporated metal; (4) atom beam; (5) water-cooled diaphragms; (6) water-cooled panel; (7) tungsten heater; (8) cathode; (9) control grid; (10) accelerating grid; (11) internal collector; (12) external collector; (13) tungsten strings; (14) electron beam; (15) removable grid for calibration plates.

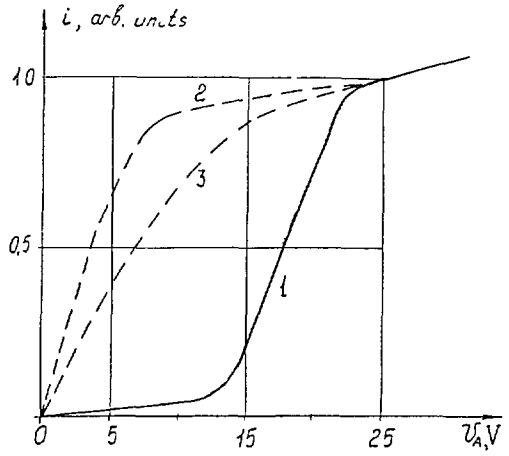

Fig. 2. — Current-voltage characteristic of low-voltage electron gun. 1-grid 2-collector 35 mm path; 2-grid 2-collector 4 mm path; 3-grid 2-collector 26 mm path (with quasi-equipotentialization strings).

preset equipotential lines, having the potential of grid 2 and external collector; curve 3 (Fig. 2) corresponds just to such a system. Geometrical transparence of this system is near 95 % for the electron beam and near 97 % for the atom beam. With equal electron energies of 10 eV and beam current density of 1 mA/cm^2 the use of quasi-equipotentialization leads to the

reduction of the collision space deviation from equipotentiality by more than a decimal order; the functioning of such a system is discussed in detail in [2]. Without quasi-equipotentialization the use of extended beams in the energy range less than 10 eV, which is especially important when investigating the excitation of metal atoms, would be senseless, since electron beam blanking by a space charge reduces its current in this region approximately by 2 orders with a corresponding decrease of the optical signal.

Another important distinction of the method of extended crossing beams from the traditional variant consists in the method calibration of the cross-sections' absolute values. As we know, the determination of the scale of the cross-sections' absolute values is usually done through substitution of a standard radiation source – a thermal radiator or hydrogen discharge tube for the source with crossing beams. The most important point, influencing the accuracy of such a substitution, is the consideration of geometric factors, that is, the geometry of the studied radiation source and that of standard radiation sources should be as much similar as possible. Obviously, the substitution of a thermal radiator with a flat radiating surface for our radiating source having a length along line of sight of the optical system 200 mm, is to a large extent incorrect. That is why, when working with extended beams in the capacity of standards for setting of the scale absolute values, the radiation of helium atoms (which are leaked in the collision space) is used instead of atoms of the studied substance while the other experimental conditions are preserved. The helium spectrum is rather convenient for such a substitution, and values of the excitation cross-sections for four lines of the helium atom, obtained in [3], have the least experimental error among well-known works. The calibration experiment is carried out with an electron energy of 50 eV, corresponding to the conditions of measurements in [3], and transition to values for other energies of electrons is done using the optical excitation functions recorded in the present paper.

The concentration of atoms of the studied metal, which should be known for determining absolute values of cross-sections with the help of the procedures described above, is found by measuring the mass of the film, condensed for a certain period of time on special calibration plates. Eight plates of titanium foil are placed perpendicular to the atom beam on a special grid (15), which during the calibration is put just behind the beam crossing region. The measurement accuracy of the film mass (approximately 1 mg) is equal to 0.01 mg. The adhesion coefficient of atoms of the most studied metals (except bismuth and lead) on the surface of the plate is actually equal to one, which is controlled by the sharpness of string shades and by the absence of redeposition of metal in shaded areas of the chamber after multi-hour operation of the plant. Atoms of metals may trap molecules of residual gases in the film as a result both of chemical and physical sorption. This is why the composition of the deposited film was analyzed by the method of X-ray-electron spectroscopy (ESCA) on the surface and in the depth of the film (after etching by the beam of argon ions) and the corresponding correction was made.

In the present work evaporated praseodymium of mark П PM-1 containing less than 0.1 % of impurity (main impurity – rare-earth metals) was placed into a tantalum crucible for formation of the atom beam. At a temperature of the metal surface equal to 1600 K the concentration of praseodymium atoms in the region of crossing of the atom and electron beams amounted to 1.9×10^9 cm^{-3}. Evaporated atoms at the above mentioned temperature may be not only in the ground state PrI $^4I^0_{9/2}$, but also as a result of thermal excitation populate sublevels of the ground state from $J = 11/2$, $13/2$, $15/2$, as well as low-lying even states. Direct control of the population of low-lying states of the praseodymium atom under the conditions of our experiment is for the time being impossible. Estimates, made on the assumption that the Boltzmann distribution is true, give the following values of population (in % of the total atom concentration in the beam): $^4I^0_{9/2}$. 65; $^4I^0_{11/2}$. 22; $^4I^0_{13/2}$. 7; $^4I^0_{15/2}$. 2.1; $^4I_{9/2}$. 1.4;

$^4K_{11/2}$. 1.1; $^4H_{9/2}$. 0.4. All the other low-lying states hardly reach a total near 1 % of the total atom concentration in the beam. Thus, approximately 90 % of atoms before collision with electrons are on two sublevels of the ground state $^4I^0_{9/2,11/2}$, separated by an interval of 1377 cm^{-1} Apparently, this distribution differs only slightly from the distribution in states of praseodymium atoms in gas-discharge plasma. Thus the values of cross-sections which we have obtained, can be used as reference data when solving problems of plasma physics. Besides, with changes in temperature the distribution of atoms in low-lying states PrI changes considerably more slowly than the total concentration of atoms.

In the course of improving the equipment and technique multiple control experiments were carried out to determine the influence of different factors on the obtained results and to optimize the conditions of the experiment. For example, when studying the role of the atom beam inhomogeneity in the collision space the control grid was sectionalized along the cathode into 12 equal sections. Each section could be connected independently or in different combinations with other sections, the absence of mutual influence being checked through the control of additivity of the current beam and of the optical signal. These measurements permitted us to determine the partial contribution of each section to the total current of the electron beam and to the resulting optical signal; one should know this for evaluating the scale of absolute values with a better accuracy since the distribution of atoms in the collision space in measurements with metals and helium is not identical.

If in a spectrogram, the peak amplitudes for spectral lines of a metal under investigation and reference gas are I_m and I_s, respectively, then the excitation cross-section of metal line is governed by a ratio:

$$Q_m = Q_s \cdot \frac{I_m}{I_s} \cdot \frac{\eta_s}{\eta_m} \frac{i_s}{i_m} \frac{n_s}{n_m} \alpha \quad , \tag{1}$$

where Q_s = excitation cross-section of helium atom line taken as a reference one; η_s and η_m = spectral sensitivity of a plant that radiates the respective lines; i_s and i_m = electron beam current at the excitation of reference gas and metal; n_s and n_m = atom concentration of reference gas and metal.

Value α is a correction factor taking into account the difference between space distributions of the metal and reference gas atoms in the collision space. For the reference gas this distribution may be considered as uniform while for the metal investigated it is determined by the above method on the basis of density of a thin film condensed on calibration plates. In the experiment with sectionalized beam at the gas target excitation, if we measure partial contribution γ_i of each section to the resulting light flux Φ to the radiation receiver, then at the metal atom excitation this light flux is

$$\Phi = \sum_{i=1}^{N} n_i \gamma_i \tag{2}$$

where i is the section number; N, the total number of sections and n_i, the metal atom concentration on the i-th section. The summation is made over all sections. The correction factor is determined from ratio

$$\alpha = \frac{\Phi_a}{\Phi_m} = \frac{\sum n_a \gamma_i}{\sum n_i \gamma_i} \quad , \tag{3}$$

where $n_a = \frac{1}{N} \sum n_i$ is the mean value of the metal atom concentrations α is the ratio of two light fluxes: Φ_a which would radiate for a uniform distribution of metal atoms in the collision space (as it does at the gas excitation) and Φ_m which is the light flux for the real distribution

measured with the same total number of atoms in the collision space. Finally, we obtain

$$\alpha = \frac{n_a \cdot \sum \gamma_i}{\sum n_i \gamma_i} = \frac{\sum n_i}{N \cdot \sum n_i \gamma_i} \quad , \tag{4}$$

since $\sum \gamma_i = 1$. Thus, by measuring the distribution of metal film density on the calibration plates in each calibration experiment it is possible to introduce the correction needed. Practically, for all metals used in the experiments, values of the correction factors differ from unity by less than 10 %; the only exception is hafnium for which $\alpha = 1.32$ has been obtained during one of the calibration procedures.

Comparison between optical excitation functions (OEF) obtained and data of other authors has also been carried out. For most metals investigated by means of the extended crossing beams, such a comparison is impossible because medium- and high-temperature metals have been for the first time investigated by us. Comparison with our results obtained after 1983 for manganese, copper, bismuth, plumbum, indium, aluminium has not shown any systematic differences from data of other authors but these is yet a rather limited amount of these data.

More detailed results of the comparison with noble gases are presented in [4, 5] but due to high excitation potentials of the noble gas atoms they do not cover a region of energies less than 10 eV. Comparison with the results of the important article of van Zyl *et al.* [3] is not very significant either since, in the latter, one did not measure OEF but cross-section values at fixed energies of 50, 100, 500, 1000, 2000 eV, and only two of these values are in the energy region studied in this work.

As follows from the results of our previous study [2], a change in the electron energy under conditions of extended beam with the use of quasi-equipotentialization results not in a change of the beam geometry in the low-energy region but, first of all, in the beam blanking due to a negative space charge. Under such conditions the sight field of spectral apparatus optical system is of not so great importance as it is in the case of conventional narrow beams. It is only important that there be no change in the sight field on scanning in a spectrum; this is achieved in this study by means of achromatic mirror optics without refraction elements. Use is made of a condenser with two spherical concave mirrors that is assembled according to a z-shaped scheme at small deviation from the normal beam incidence; the latter is required to reduce aberrations. A monochromator with diffraction grids of 600 and 1200 lines/mm also contains only mirror elements. In special experiments carried out using a method with two successive identical monochromators, the spectral transmission of the whole optical system (quartz windows of the vacuum chamber included) has been measured for two mutually perpendicular states of the linear polarization of radiation as well as of the spectral sensitivity of photomultipliers. A detailed description of other control experiments in the present paper seems irrelevant.

3. Results of the measurements and their discussion.

82 spectral line cross-sections of the praseodymium atom, lying in the spectrum region of 349...569 nm were measured at an energy of exciting electrons of 30 eV. The dependence of the excitation cross-sections on the energy of the exciting electrons (optical excitation functions, OEF) have been measured in the energy range of 0...200 eV for approximately half of the total number of cross-sections.

Table I. — *Effective excitation cross-sections of praseodymium atom.*

λ nm	Transition		J	E_L cm^{-1}	E_U cm^{-1}	Q_{30} 10^{-18} cm^{-2}	Q_{max} 10^{-18} cm^{-2}	E(max) eV	OEF
1	2		3	4	5	6	7	8	9
349.149	–		–	–	–	13.2	–	–	–
448.858	$(4f^36s^2\ ^4I^o$ –	?	9/2 – 7/2	0	22272)	35.2	40.0	50	31
453.233	$(4f^36s^2\ ^4I^o$ –	?	9/2 – 7/2	0	22058)	29.9	34.0	40	30
454.126	$(4f^36s^2\ ^4I^o$ –	?	9/2 – 7/2	0	22014)	49.3	60.5	48	29
455.226	$4f^36s^2\ ^4I^o$ –	?	9/2 – 7/2	0	21961	149	186	45	28
457.214	$4f^36s^2\ ^4I^o$ –	$4f^36s6p\ ^4G'$	11/2 – 9/2	1377	23242	35.7	43.5	50	36
460.258	$(4f^36s^2\ ^4I^o$ –	?	9/2 – 7/2	0	21721)	17.2	–	–	–
461.773	$4f^36s^2\ ^4I^o$ –	?	9/2 – 7/2	0	21650	45.8	57.7	45	25
463.228	$4f^36s^2\ ^4I^o$ –	?	15/2 – 13/2	4381	25963	22.0	–	–	–
463.569	$4f^36s^2\ ^4I^o$ –	?	9/2 – 7/2	0	21566	190	206	17	23
463.956	$4f^36s^2\ ^4I^o$ –	?	11/2 – 9/2	1377	22924	116	124	20	35
466.091	–		–	–	3.0 ± 0.5	31.7	33.6	80	39
467.479	$(4f^36s^2\ ^4I^o$ –	?	11/2 – 9/2	1377	22762)	75.8	79.0	16	34
468.781	–		–	–	2.8 ± 0.5	73.1	86.0	75	40
469.577	$(4f^36s^2\ ^4I^o$ –	?	13/2 – 11/2	2847	24137)	67.8	71.1	20	37
471.307	$4f^36s^2\ ^4I^o$ –	?	9/2 – 7/2	0	21212	123	148	50	21
472.261	–		–	–	–	15.9	–	–	–
473.069	$4f^36s^2\ ^4I^o$ –	?	11/2 – 9/2	1377	22509	120	120	30	33
473.669	$4f^36s^2\ ^4I^o$ –	?	9/2 – 7/2	0	21106	313	326	17	19
474.416	$4f^36s^2\ ^4I^o$ –	?	9/2 – 7/2	0	21073	149	154	22	18
476.781	–		–	–	3.5 ± 0,5	29.0	33.5	80	41
477.456	$(4f^36s^2\ ^4I^o$ –	?	9/2 – 9/2	–	20939)	20.7	–	–	–
477.546	–		–	–	–				
478.832	$4f^36s^2\ ^4I^o$ –	?	9/2 – 9/2	0	20878	17.6	–	–	–
479.875	–		–	–	–	18.9	–	–	–
480.825	$4f^36s^2\ ^4I^o$ –	?	9/2 – 7/2	0	20792	58.1	59.3	23	16
481.110	$(4f^36s^2\ ^4I^o$ –	?	11/2 – 13/2	1377	22156)	17.2	–	–	–
483.933	–		–	–	–				
484.051	$(4f^36s^2\ ^4I^o$ –	?	9/2 – 7/2	0	20653)	31.4	44.8	45	15
484.078	–		–	–	–				

1	2	3	4	5	6	7	8	9
484.811	$(4f^36s^2\ ^4I^o$ – ?	9/2 – 9/2	0	20621)	14.1	–	–	–
485.371	$4f^25d6s^2\ ^4I^o$ – ?	9/2 – ?	4432	25029	20.2	–	–	–
487.013	–	–	–	–	17.0	–	–	–
488.226	$4f^36s^2\ ^4I^o$ – ?	9/2 – 9/2	0	20477	59.0	60.2	25	13
488.671	–	–	–	–	11.4	–	–	–
489.610	$4f^36s^2\ ^4I^o$ – ?	11/2 – 9/2	1377	21795	56.4	58.7	20	27
490.698	$4f^36s^2\ ^4I^o$ – ?	15/2 – 15/2	4381	24754	31.7	–	–	–
491.403	$4f^36s^2\ ^4I^o$ – ?	9/2 – 9/2	0	20344	252	263	20	12
491.541	–	–	–	–	17.2	–	–	–
492.459	$4f^36s^2\ ^4I^o$ – ?	11/2 – 11/2	1377	21677	228	232	25	26
493.215	$4f^36s^2\ ^4I^o$ – ?	9/2 – 7/2	0	20269	77.5	–	–	–
493.600	$4f^36s^2\ ^4I^o$ – ?	15/2 – 15/2	4381	24635	22.0	–	–	–
493.974	$4f^36s^2\ ^4I^o$ – $4f^36s6p\ ^4I$	13/2 – 13/2	2847	23085	224	257	16	24
494.030	$4f^36s^2\ ^4I^o$ – ?	11/2 – 11/2	1377	21613				
495.136	$4f^36s^2\ ^4I^o$ – $4f^36s6p\ ^4I$	9/2 – 9/2	0	20191	722	803	16	16
495.606	$4f^36s^2\ ^4I^o$ – ?	9/2 – 11/2	0	20172	38.7	–	–	–
496.017	$4f^36s^2\ ^4I^o$ – ?	9/2 – 9/2	0	20155	121	164	45	10
496.097	–	–	–	–			–	–
497.097	–	–	–	–	16.3	–	–	–
497.494	$4f^36s^2\ ^4I^o$ – ?	11/2 – 11/2	1377	21472				
497.579	$4f^36s^2\ ^4I^o$ – ?	15/2 – 15/2	4381	24473	277	305	18	9
497.641	$4f^36s^2\ ^4I^o$ – ?	9/2 – 11/2	0	20089				
500.765	$(4f^36s^2\ ^4I^o$ – ?	9/2 – 9/2	0	19964)	34.4	35.8	18	8
501.858	$4f^36s^2\ ^4I^o$ – ?	9/2 – 11/2	0	19920	270	282	18	7
501.976	$4f^36s^2\ ^4I^o$ – $4f^36s6p\ ^4K$	13/2 – 15/2	2847	22763				
502.697	$4f^36s^2\ ^4I^o$ – $4f^36s6p\ ^4K$	11/2 – 13/2	1377	21264	197	207	18	22
503.311	–	–	–	–	136	141	–	–
503.339	$4f^36s^2\ ^4I^o$ – ?	9/2 – 11/2	0	19862			20	6
504.383	$4f^36s^2\ ^4I^o$ – ?	9/2 – 11/2	0	19821	264	271	18	5
504.553	$4f^36s^2\ ^4I^o$ – $4f^36s6p\ ^4K$	15/2 – 17/2	4381	24195	52.8	56.3	18	38
505.340	$4f^36s^2\ ^4I^o$ – ?	11/2 – 13/2	1377	21160	121	127	20	20
506.289	–	–	–	–	30.4	–	–	–
506.340	$4f^36s^2\ ^4I^o$ – ?	11/2 – 11/2	1377	21121				
507.241	–	–	–	–	12.7	–	–	–

1	2	3	4	5	6	7	8	9
508.711	$4f^36s^2\,{}^4I^o$ – ?	13/2 – 15/2	2847	22499	62.0	77.5	60	32
511.732	–	–	–	–	21.5	–	–	–
513.342	$4f^36s^2\,{}^4I^o$ – $4f^36s6p\,{}^4I$	9/2 – 11/2	0	19475	488	519	16	4
513.982	$4f^36s^2\,{}^4I^o$ – ?	11/2 – 13/2	1377	20827	66.0	67.6	25	17
514.748	$4f^36s^2\,{}^4I^o$ – ?	11/2 – 13/2	1377	20798	19.4	–	–	–
515.680	–	–	–	–	16.7	–	–	–
516.832	$4f^36s^2\,{}^4I^o$ – ?	9/2 – 11/2	0	19343	52.0	52.0	30	3
517.737	$4f^36s^2\,{}^4I^o$ – ?	13/2 – 13/2	2847	22156	15.8	–	–	–
517.838	–	–	–	–				
518.345	–	–	–	–	12.3	–	–	–
519.441	$4f^36s^2\,{}^4I^o$ – ?	11/2 – 13/2	1876	20623	146	146	30	14
522.801	$4f^36s^2\,{}^4I^o$ – ?	9/2 – 11/2	0	19123	172	179	20	2
525.313	–	–	–	–	16.3	–	–	–
531.656	–	–	–	–	26.4	–	–	–
532.499	–	–	–	–	15.8	–	–	–
534.200	–	–	–	–				
534.285	–	–	–	–	18.5	–	–	–
534.365	–	–	–	–				
539.583	–	–	–	–	14.5	–	–	–
542.027	$(4f^36s^2\,{}^4I^o$ – ?	11/2 – 11/2	1377	19821)	21.6	22.2	18	5
542.236	$4f^35d6s\,{}^6K$ – ?	9/2 – 11/2	8320	26757			–	–
543.289	$4f^36s^2\,{}^4I^o$ – ?	9/2 – 7/2	0	18401	46.7	–	–	–
546.027	$4f^36s^2\,{}^4I^o$ – ?	9/2 – 11/2	0	18309	97,0	101	33	1
546.949	–	–	–	–	29.9	–	–	–
546.990	$4f^35d6s\,{}^2L^o$ – ?	11/2 – 11/2	8080	26357				
548.176	$4f^36s^2\,{}^4I^o$ – ?	9/2 – 11/2	0	18237	33.4	–	–	–
552.389	$(4f^36s^2\,{}^4I^o$ – $4f^36s6p\,{}^4I$	11/2 – 11/2	1377	19475)	53.7	57.2	16	4
556.005	$(4f^36s^2\,{}^4I^o$ – ?	13/2 – 13/2	2847	20827)			25	17
556.113	$(4f^35d6s\,{}^6L^o$ – ?	13/2 – 13/2	8733	26710)	38.7	39.7	–	–
556.230	$(4f^35d6s\,{}^2L^o$ – ?	15/2 – 15/2	9647	27620)			–	–
556.902	$(4f^36s^2\,{}^4I^o$ – ?	13/2 – 13/2	2847	20798)	63.4	–	–	–
559.271	–	–	–	–	44.9	–	–	–
566.344	–	–	–	–	58.1	–	–	–
567.222	–	–	–	–	64.3	–	–	–
568.742	$(4f^36s^2\,{}^4I^o$ – $4f^36s6p\,{}^4K$	9/2 – 11/2	0	17578)	54.6	–	–	–

Our results are given in table I. They include wavelength, transition, values of the full moment quantum number, energy of upper and lower levels counted off from the atom ground state, excitation cross-sections with electron energy of 30 eV and at the OEF maximum, position of the maximum and OEF number according to curve numbering in Figure 3a-e. Measured values of threshold energy indicate the absence in the beam of metastable atoms in quantities that can be detected and agree only with the possibility of the praseodymium atom excitation from the states $^4I^0_{9/2,\ 11/2}$. OEF have been measured also for three comparatively intensive unclassified PrI lines; for these lines the values of threshold energy are given in eV in column "E_U"

Figure 4 presents a spectrogram region that includes praseodymium atom lines. The electron energy is 30 eV, the spectrum scanning velocity is 4.0 nm/min, and the characteristic time of the recording system is 2.0 s. The real spectral resolution under such conditions is about 1.5 to 2.0 Å but, if required, it may be improved up to 1.0 Å and for the most intensive lines up to 0.5-0.6 Å. A main factor that controls the real spectral resolution under the conditions of this experiment is the relation of the characteristic time of recording system to the spectrum scanning velocity while the monochromator spectral resolution is not wholly employed. It is to be noted that the spectral resolution achieved in this work is higher than that obtained by most investigators using the method of crossing beams. However it does not always allow resolution of the spectral lines of the rare-earth element atoms because their spectra are abounding in lines.

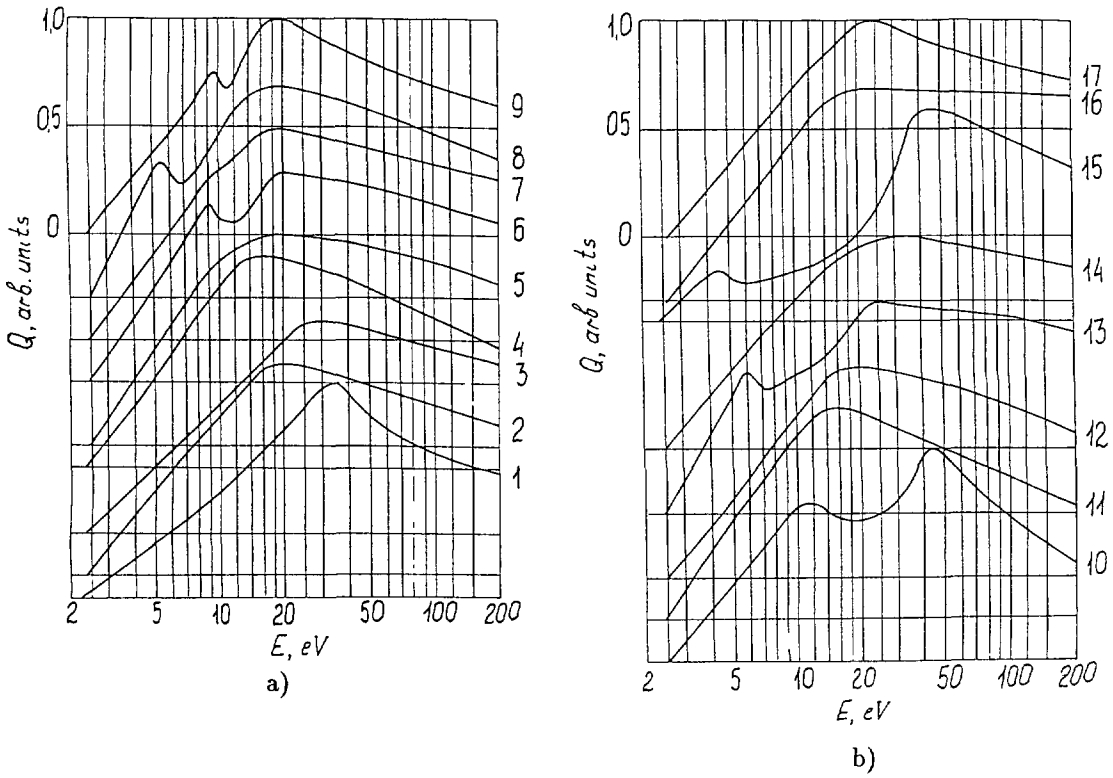

Fig. 3a-e. — Optical excitation functions of praseodymium atom.

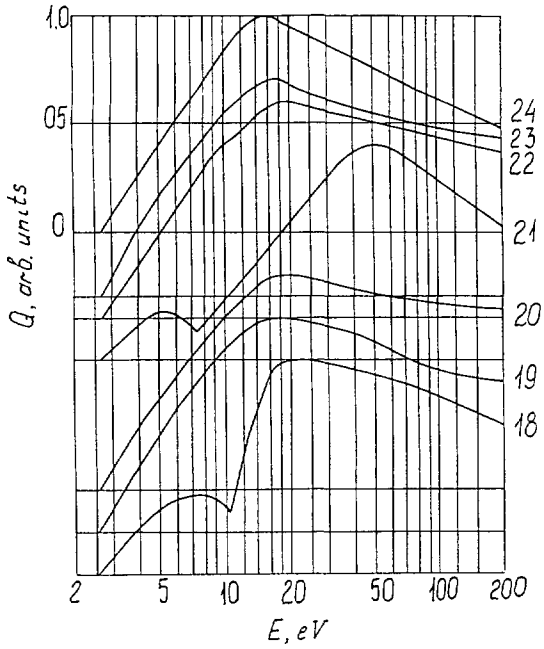

c)

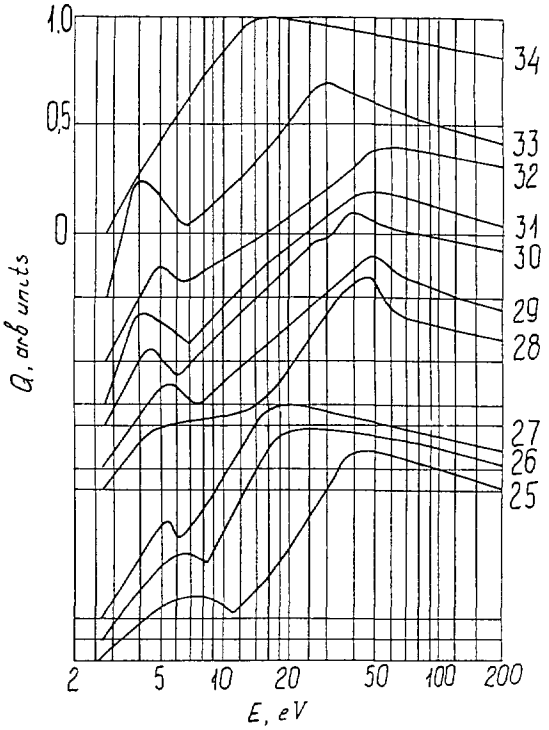

d)

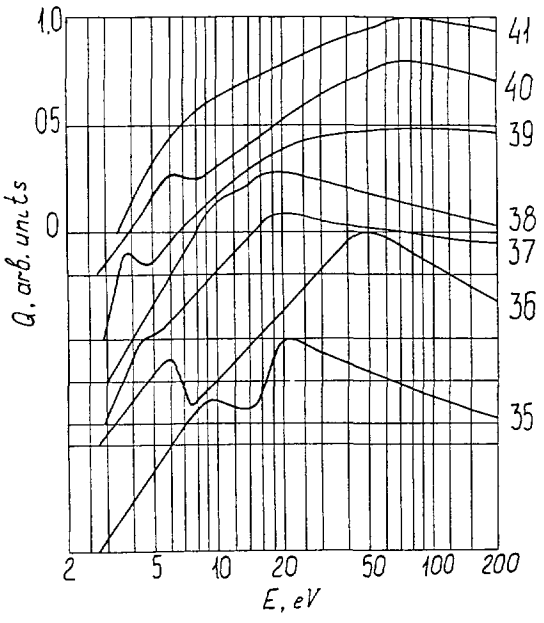

e)

Fig. 3. — (*continued*)

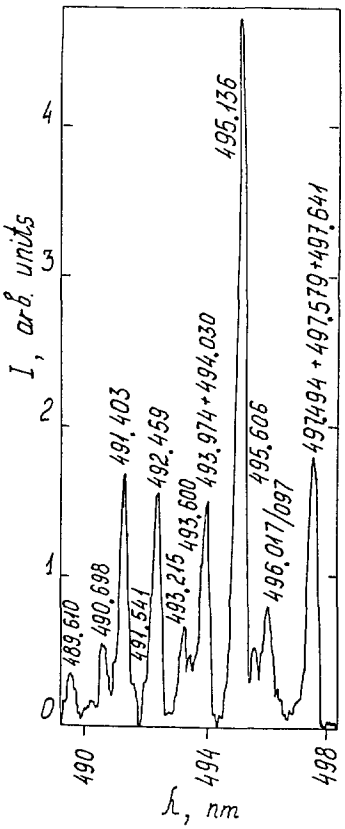

Fig. 4. — Praseodymium atom spectrum region.

The spectral line identification has been carried out using data of [6]; use was also made of additional information from [7]. Classification of PrI spectral lines is given in accordance with detailed papers [6, 8] (excluding 542.236 and 543.289 nm for which [9] has been used). In [4] are not mentioned a number of PrI lines which, when excited by a beam of monokinetic electrons, have a comparatively high intensity. Measurements of threshold energy indicated that these lines appear as a result of transitions of the praseodymium atom to low-lying states and are often resonant. On the base of this information and using values of terms from [8] a classification has been made for 18 PrI lines lying in the spectrum region 448...569 nm. The corresponding results are given in table I in brackets. During classification it was considered necessary to satisfy the following requirements: different parity of upper and lower states; observance of the selection rule $\Delta J = 0, \pm 1$, and deviation of wavelength (calculated on the basis of the level energy values) from spectroscopic values smaller than $(2\text{-}3) \times 10^{-3}$ nm. 8 lines out of newly classified ones turned out to ne resonant; for only 2 lines the full set of quantum numbers in upper states is known.

The measured PrI excitation cross-sections are comparatively large; they lie in the range $10^{-17}.. 10^{-15}$ cm^2, the cross-sections of 22 lines exceeding 10^{-16}cm^2 at the maximum OEF. The largest of these values amounting to $(5...8) \times 10^{-16}$ cm^2, correspond to two resonant transitions in multiplet $4f^36s^2\ {}^4I^0$ and $4f^36s6p\ {}^4I$.

A considerable part of recorded OEF has peculiarities in the form of breaks or second maxima, but we cannot interpret them at present both because of the absence of any theoretical work on the excitation of the praseodymium atom and because of the fact that for almost all upper PrI levels, only the energy values and J are known. According to [8] in the spectrum region 0.4...1.2 μm about 25000 spectral lines PrI are known, but nearly all of them are unclassified.

The experimental error in determining the cross-section relative values is $\pm$ 15 to $\pm$ 23% depending on the intensity of the line and spectrum region where the latter occurs. The error in determining the cross-section absolute values ranges from $\pm$ 25 to $\pm$ 35%, but this does not take into account the polarization state of lines under investigation. Causes for the experimental errors in the extended crossing beam experiments are discussed in more detail in [5].

References

[1] Smirnov Yu.M., Physics of electron and atom collisions (PhTI AS USSR. Leningrad, 1985) pp.183-193.

[2] Kuchenev A.N., Samsonova Ye.A., Smirnov Yu.M., *Autometry* No. 5 (1990) 109-113.

[3] Van Zyl B., Dunn G.H., Chamberlain G. and Heddle D.W.O., *Phys. Rev.* **A22** (1980) 1916-1929.

[4] Smirnov Yu.M., *Astron. J.* (USSR) **61** (1984) 1087-1097.

[5] Smirnov Yu.M., Effective cross-sections for electron-impact excitation of atoms and ions (Standard Publishing House. Moscow, 1989) p.265.

[6] Meggers W.F., Corliss C.H., Scribner B.F., Tables of spectral lines intensities. NBS (US), Mono 145. Part. 1 (1975) pp. 203-215.

[7] Zalubas R., Wilson M., *J. Res. NBS* **69A** (1965) 59-70.

[8] Martin W.C., Zalubas R., Hagan L., Atomic energy levels. The rare earth elements, NBS (US) (1978) 95-101.

[9] Ginibre A., *Phys. Scr.* **23** (1981) 260-267.